Journal of Applied Physics

# High-density magneto-optical disk storage and the effect of finite beam size in readout

Cite as: Journal of Applied Physics **56**, 1165 (1984); https://doi.org/10.1063/1.334044
Submitted: 30 January 1984 . Accepted: 04 April 1984 . Published Online: 04 June 1998

M. Mansuripur

# High-density magneto-optical disk storage and the effect of finite beam size in readout

M. Mansuripur
*Boston University, College of Engineering, Boston, Massachussetts*

(Received 30 January 1984; accepted for publication 4 April 1984)

A method of data reconstruction from a digital magneto-optical disk system with diffraction-limited spot size is described. Using a linear filter with high-frequency enhancement we show that significant improvements in the storage capacity can be achieved at a reasonable cost in terms of the signal-to-noise ratio. Performance is evaluated against an optimum but impractical method as well as a technique for the reconstruction of the analog waveforms.

## I. INTRODUCTION

In comparison with the conventional magnetic disk systems, erasable optical storage has the advantages of high capacity, remote read/write/erase heads, and removability.[1,2] Among those media suggested for erasable optical storage to date, amorphous rare-earth-transition metal alloys with perpendicular magnetization have shown great promises.[3] With thermomagnetic recording and magneto-optical readout at red or near infrared wavelengths, densities in excess of $10^8$ bits/cm$^2$ have been achieved.

A significant difference between magnetic and optical recording techniques stems from the fact that in the former the readout energy is derived from the magnetic domains themselves, whereas in the latter the domains act as gates, directing the energy of the reading light beam into separate channels for detection. This means that the magnetic recording density is inherently limited while the optical recording density is only limited by the wavelength of the available lasers.

Optical storage is presently limited by the wavelength of the read beam. The diffraction limited spot formed by focusing a gaussian beam of wavelength $\lambda$ through an objective lens of numerical aperature $NA$ is gaussian, and has a diameter proportional to $\lambda/NA$. Increasing the storage density for a given spot size results in reduced signals from individual domains and overlapped signals from neighboring domains, a phenomenon referred to as the intersymbol interference (ISI). Both reduced signal and overlap degrade the signal-to-noise ratio (SNR) and impose limitations on achievable storage densities. It is important to emphasize here that ISI results from the read beam overlapping more than one domain and not magnetic coupling between domains. In fact, since most media of interest for erasable optical storage are ferrimagnetic with compensation point in the vicinity of room temperature, magnetic coupling between neighboring domains should be insignificant.

The aim of this paper is to discuss different signal processing schemes that can recover data from a high density storage medium in the presence of ISI. In Sec. II the various components and parameters of the proposed readout system are described. Section III is devoted to the analysis of the three suggested techniques for data reconstruction. Section IV is a summary of the results and contains a few general comments and conclusions.

## II. MAGNETO-OPTICAL READOUT AND DIFFERENTIAL DETECTION SCHEME

The schematic diagram of the readout system is shown in Fig. 1; this section describes its components and defines various parameters and functions that will be used throughout the paper.

### A. The storage format

The disk contains a magnetic layer with perpendicular magnetization on which the information is recorded in the form of small magnetic domains. Assuming that the magnetization of the film at a point $(\rho,\theta)$ is saturated in either of the two possible directions along the $Z$ axis, the function $z(\rho,\theta)$ is defined as follows: $z(\rho,\theta) = \pm 1$ if the magnetization at $(\rho,\theta)$ is in the $\pm Z$ direction. The read beam reads only one particular track at any given time, so only the neighborhood near a fixed radius, say $\rho = \rho_0$, is of interest. The sequence of data on this track can then be represented as $z(x)$ where $x = \rho_0\theta$ is

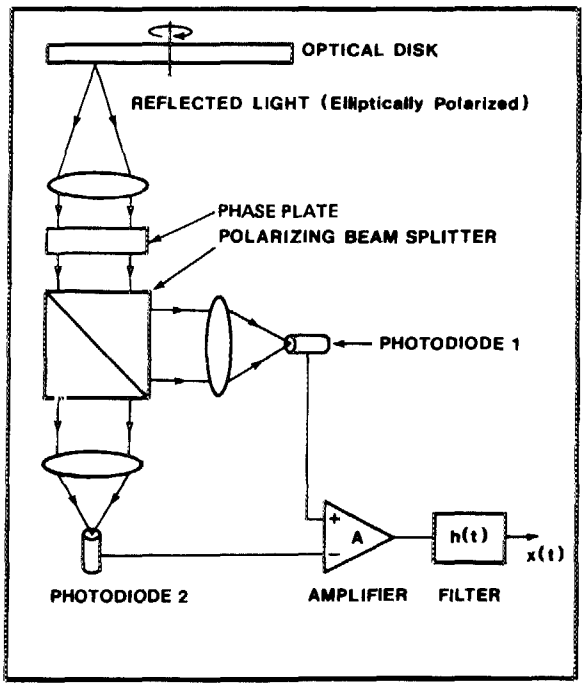


FIG. 1. Schematic diagram of the magneto-optical readout system.

 0021-8979/84/161165-06$02.40  

the distance along the track from an arbitrary reference angle. Assume that the length of the domains in the $x$ direction is a constant $\gamma$. If the linear velocity of the track is $v$, then the time each domain spends under the beam will be $T = \gamma/v$. It is assumed that $T$ is a fixed system parameter, so that comparisons of the next section between different techniques are made at fixed data rates.

The ideal signal, expected from the system in the absence of noise and ISI, is $z_0(t) = z(vt)$. Using the rectangular pulse function $s(t)$ of unit height and duration $T$, this signal can be written as

$$z_0(t) = \sum_n a_n s(t - nT), \tag{1}$$

where $a_n = \pm 1$ and $\{a_n\}$ represents the binary sequence of data recorded on the track.

### B. The read beam

The beam is focused on the disk surface through the objective lens. The intensity distribution on the film is assumed to be gaussian with

$$I(x,y) = \frac{P_0}{\pi r_0 r_1} \exp\{-[(x/r_0)^2 + (y/r_1)^2]\}. \tag{2}$$

$r_0$ is the beam radius in the $X$ direction (along the track), $r_1$ is the radius in the $Y$ direction (perpendicular to the track), and $P_0$ is the total incident power. Throughout the paper it is assumed that in the $Y$ direction the domain width is much larger than $r_1$ so that the intensity distribution in this direction becomes irrelevant. One can then use the function

$$g(x) = \frac{P_0}{\sqrt{\pi} r_0} \exp[-(x/r_0)^2] \tag{3}$$

to represent the incident power density on the track.

The read beam is linearly polarized. Upon reflection from the magnetic material its state of polarization will change. This is the well-known polar Kerr effect. In general, two parameters $r_\parallel$ and $r_\perp$ describe the new polarization state. $r_\parallel$ is the amplitude reflectivity for the component polarized in the direction of incident polarization and $r_\perp$ is the amplitude reflectivity for the component perpendicular to it. Both $r_\parallel$ and $r_\perp$ are complex numbers and the phase difference between them determines the amount of ellipticity. Nonetheless, with proper adjustment of the phase plate (see Fig. 1) this phase difference can be eliminated, converting ellipticity to pure rotation of the direction of linear polarization. Since the system does not detect ellipticity the above conversion improves performance.[4,5] $r_\parallel$ and $r_\perp$ are thus assumed to be real.

### C. The optical system

The axis of the polarizing beam splitter is at 45 deg with respect to the unrotated polarization so that in the absence of the polar Kerr effect the photodiodes receive identical amounts of energy ($0.5P_0 r_\parallel^2$). When the Kerr effect is present the energy is split as $0.5P_0(r_\parallel \pm r_\perp)^2$ between the two detectors, with the state of magnetization determining the detector which receives the larger amount. The difference between these energies, $2P_0 r_\parallel r_\perp$, gives the magneto-optic signal amplitude while their sum, $P_0(r_\parallel^2 + r_\perp^2)$, is proportional to the total shot-noise density.[4]

### D. The electronic circuitry

The photodiodes are identical light detectors with conversion factor $\eta$. Each photocurrent goes through a parallel $RC$ circuit before being amplified. The $RC$ circuit represents the impedances of the detector, the amplifier, and the bias circuitry. Its frequency response is $RH_0(f)$ where

$$H_0(f) = 1/(1 + j2\pi RCf). \tag{4}$$

The effect of thermal noise from the electronic circuitry is minimized if avalanche detectors with internal gain mechanism are employed. SNR analysis is thus confined to shot noise although thermal noise can be easily included if so desired. The shot-noise variance is independent of the state of magnetization and is given by[4]

$$\sigma^2 = \eta e P_0(r_\parallel^2 + r_\perp^2) \int_{-\infty}^{\infty} |H_{eq}(f)|^2 df, \tag{5}$$

where $e$ is the electronic charge and $H_{eq}(f)$ is the frequency response of the equivalent filter. If $H(f)$ represents the frequency response of the filter $h(t)$ in Fig. 1 then

$$H_{eq}(f) = H_0(f)\, H(f). \tag{6}$$

Equation (5) does not include gain factors such as $R$, amplifier gain, and avalanche gain that cancel out in the SNR. When avalanche photodiodes are used, however, a noise factor due to the random nature of the multiplication process must be included.

## III. EFFECT OF INTERSYMBOL INTERFERENCE ON READOUT

As mentioned in the introduction, the nonzero read beam size is responsible for ISI. When the beam travels along the track, it illuminates an area whose length is approximately $4r_0$ (about 99.5% of the beam's energy is contained in this region). If the domain size $\gamma$ is smaller than this length there will be some degree of overlap between the signals from neighboring domains. Moreover, when the beam crosses the boundary between adjacent domains it sends back a signal which represents both domains, producing ISI. The degrading effect of this phenomenon as well as three different methods of eliminating the problem are discussed in this section.

### A. Elimination of ISI by spatial filtering: An optimum technique

This approach is based on a method which could eliminate ISI in principle, but requires an objective lens with an impractically large numerical aperture. Besides, if a large numerical aperture were available in the first place, the spot size would have been reduced and the problem eliminated. The technique nonetheless provides a yardstick for the evaluation of other methods.

The time allocated to each domain for readout is $T$ and the read beam in an optimum system must spend *all* of this time on the domain. In other words, the beam must jump from the center of one domain to the center of the next domain on the track every $T$ seconds and remain stationary in

the meantime. Now, consider the pattern of polarization at the disk during each $T$ second interval. With a high quality imaging system this pattern can be exactly reconstructed in another plane. To eliminate ISI, a spatial filter is placed in this plane, transmitting the image of the domain under consideration and blocking the image of neighboring domains. The method is optimal since all the information about a domain is contained in the light reflected from the domain itself and by blocking the neighboring domains no information is being lost.

Beyond the spatial filter, the optimum detection scheme will be the same as the differential detector of Fig. 1. The output signal amplitude is thus given by

$$\pm 2\eta r_{\parallel} r_{\perp} \int_{-\gamma/2}^{\gamma/2} g(x)dx = \pm 4\eta P_0 r_{\parallel} r_{\perp} \operatorname{erf}\left(\frac{\gamma}{\sqrt{2}r_0}\right). \quad (7)$$

The spectral density of the accompanying shot noise is given by

$$2\eta e P_0 (r_{\parallel}^2 + r_{\perp}^2) \operatorname{erf}\left(\frac{\gamma}{\sqrt{2}r_0}\right). \quad (8)$$

For the sake of optimum detection, the system impulse response $h_{eq}(t)$ must be a rectangle of duration $T$. Since the bandwidth of this filter is $2B = 1/T$ the signal-to-noise ratio is given by

$$\mathrm{SNR} = \frac{4\eta P_0 T r_{\parallel}^2 r_{\perp}^2}{e(r_{\parallel}^2 + r_{\perp}^2)} \left[2\operatorname{erf}\left(\frac{\gamma}{\sqrt{2}r_0}\right)\right]. \quad (9)$$

A logarithmic plot of the function $2\operatorname{erf}(\gamma/\sqrt{2}r_0)$ vs $\gamma/r_0$ is shown in Fig. 2. For large $\gamma/r_0$ the SNR is at its maximum possible value. This is because the beam completely covers the domain under consideration while no time is spent crossing the boundary between domains. At $\gamma = 3r_0$ where 96.5% of energy covers the domain the SNR deterioration is only 0.15 dB. At $\gamma = r_0$ the coverage is about 50% and the SNR drop is about 3 dB.

### B. Reconstruction of the pattern of magnetization reversals: The analog signal approach

In a previous paper[4] the power spectral density of the signal $x(t)$ in the system of Fig. 1 was derived. It is given by

$$S(f) = (2\eta P_0 r_{\parallel} r_{\perp})^2 \exp[-2(\pi f r_0/v)^2] \times S_{z0}(f)\,|H_{eq}(f)|^2, \quad (10)$$

where $S_{z0}(f)$ is the spectrum of the ideal signal $z_0(t)$ in Eq. (1) and is given by[6]

$$S_{z0}(f) = T\left(\frac{\sin(\pi f T)}{\pi f T}\right)^2. \quad (11)$$

Let us choose $h(t)$ to make the equivalent filter $h_{eq}(t)$ an ideal low pass filter with bandwidth $2B = \alpha/T$ where $\alpha$ is an arbitrary constant. Then

$$\mathrm{SNR} = \frac{4\eta P_0 T r_{\parallel}^2 r_{\perp}^2}{e(r_{\parallel}^2 + r_{\perp}^2)} \left\{(2/\pi\alpha) \int_0^{\pi\alpha/2} \exp[-2(r_0 x/\gamma)^2] \times (\sin x/x)^2 dx\right\}. \quad (12)$$

Figure 3 is a logarithmic plot of the bracketed term in Eq. (12) versus $\gamma/r_0$ for several values of $\alpha$. For large $\gamma/r_0$ the ISI is negligible and the signal reconstruction is possible through the use of a sufficiently wide band filter (i.e., large $\alpha$). However, as $\alpha$ increases the noise level rises and consequently the SNR drops. For small $\gamma/r_0$ the signal at any instant of time contains information about several domains and identification of individual data bits is impossible without further equalization. The issue of equalization, however, will not be addressed here since the subject of analog signal reconstruction and the enhancement of storage capacity using various encoding schemes is beyond the scope of this paper and will be taken up in a separate publication. The point of the discussion here is that for large $\gamma/r_0$ the loss of SNR in the analog approach is signficant and it is reasonable therefore to expect that such inefficiency applies to small $\gamma/r_0$ as well. For example, the SNR loss of the analog method for $\alpha = 2$ and large $\gamma/r_0$ is about 3.5 dB compared to only 0.5 dB for the digital method described below.

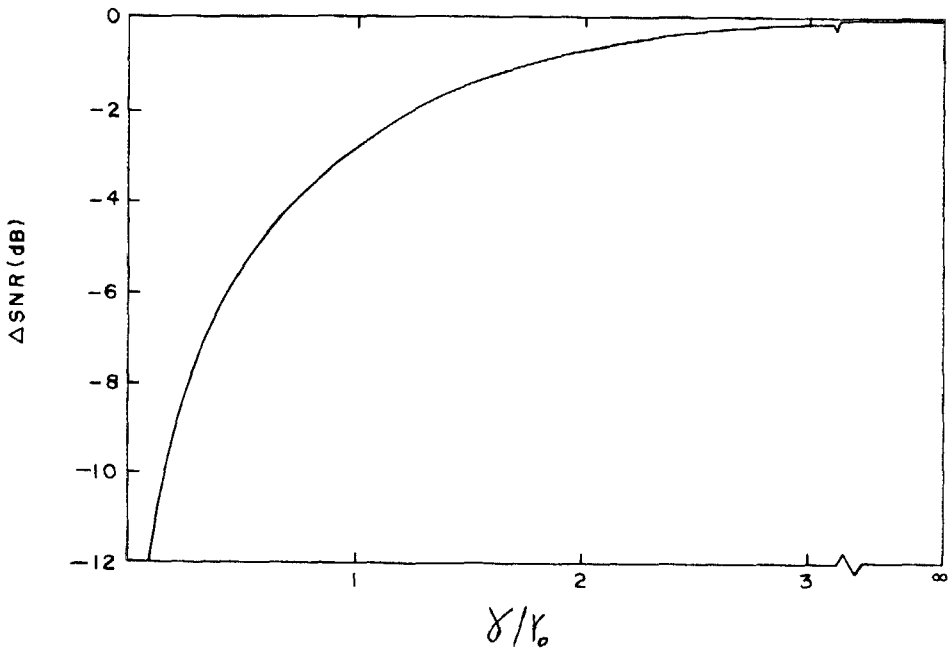


FIG. 2. Logarithmic plot of the function $2\operatorname{erf}(\gamma/\sqrt{2}r_0)$ vs $\gamma/r_0$.

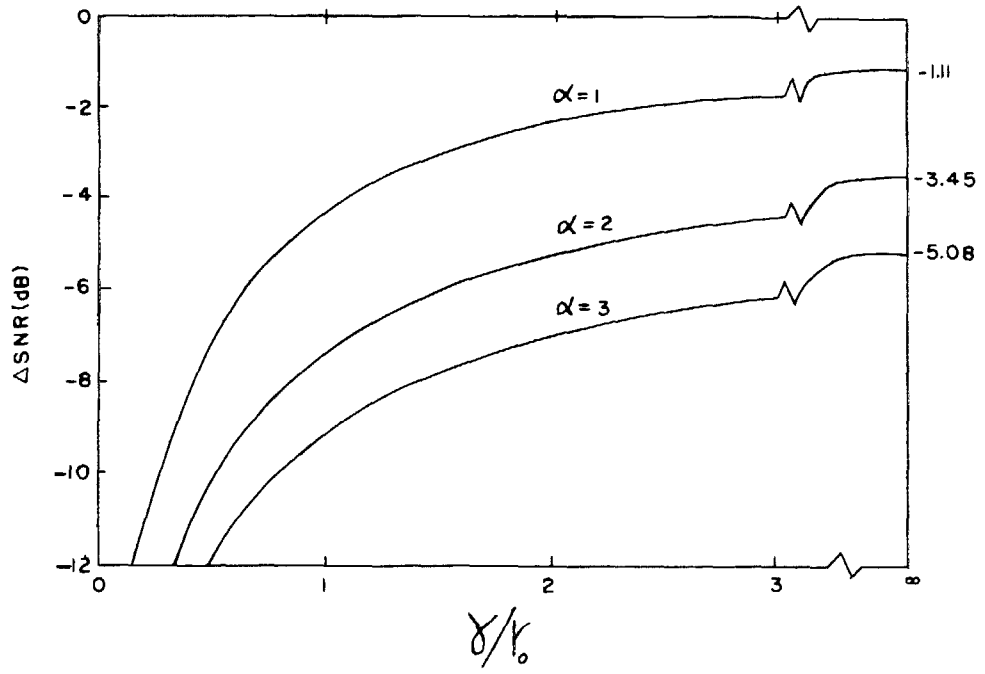


FIG. 3. Logarithmic plot of the function $(2/\pi\alpha)\int_0^{\pi\alpha/2}\exp[-2(r_0x/\gamma)^2]\times(\sin x/x)^2dx$ vs $\gamma/r_0$ for several values of $\alpha$.

### C. The digital signal approach to the elimination of ISI

In this approach the filter $h(t)$ is designed to eliminate interference only at instants of time which are multiples of $T$, namely $t=nT$. This allows a simple threshold device to sample $x(t)$ at $t=nT$ and reconstruct the sequence of data $\{a_n\}$. SNR at $t=nT$ is then a direct measure of the error rates involved.

Consider the instantaneous power $P(t)$ incident on the detectors

$$P(t)=\frac{1}{2}P_0(r_\parallel^2+r_\perp^2)\pm r_\parallel r_\perp\int_{-\infty}^{\infty}g(vt-x)z(x)dx, \quad (13)$$

where $g(x)$ is defined in Eq. (3). Defining

$$g_0(t)=\frac{\gamma}{\sqrt{\pi}r_0T}\exp\left[-\left(\frac{\gamma t}{r_0T}\right)^2\right] \quad (14)$$

the integral in Eq. (13) can be written as $P_0g_0(t)*z_0(t)$, where * stands for convolution. The output signal will then be

$$\begin{aligned}x(t)&=2\eta P_0r_\parallel r_\perp g_0(t)*z_0(t)*h_{eq}(t)\\&=2\eta P_0r_\parallel r_\perp\sum_n a_n q(t-nT),\end{aligned} \quad (15)$$

in which $q(t)$ is given by

$$q(t)=s(t)*g_0(t)*h_0(t)*h(t). \quad (16)$$

If $q(t)$ is now chosen to be equal to 1 at $t=0$ and equal to zero at $t=mT$ for all $m\neq 0$, then for $t=nT$ we have

$$x(nT)=2\eta P_0r_\parallel r_\perp a_n. \quad (17)$$

This signal clearly contains information about $a_n$ without interference from the rest of the sequence.

A proper choice of $q(t)$ would be the following family of the so called raised cosine functions[7]

$$q(t)=\frac{\sin(\pi t/T)}{\pi t/T}\,\frac{\cos(\pi\beta t/T)}{1-(2\beta t/T)^2}, \quad (18)$$

where $\beta$ is a parameter in the interval [0,1]. The Fourier transforms of the functions $s(t)$, $g_0(t)$, and $q(t)$ are given in Table I. Using these transforms in Eq. (16) yields

$$H(f)=\frac{Q(f)}{S(f)\,G_0(f)\,H_0(f)}. \quad (19)$$

This is the frequency response of the appropriate filter. A plot of $H(f)$ for typical parameter values is shown in Fig. 4.

Using the noise variance given in Eq. (5), the signal-to-noise ratio at $t=nT$ is calculated as

TABLE I. Fourier transforms of $s(t)$, $g_0(t)$, and $q(t)$.

| Function | Fourier transform |
|---|---|
| $s(t)$ | $S(f)=T\frac{\sin(\pi Tf)}{\pi Tf}$ |
| $g_0(t)$ | $G_0(f)=\exp\left[-\left(\frac{\pi Tf}{\gamma/r_0}\right)^2\right]$ |
| $q(t)$ | $Q(f)=\begin{cases}T & 0\le\lvert f\rvert\le\frac{1-\beta}{2T}\\ \frac{T}{2}\{1-\sin[\pi(Tf-0.5)/\beta]\}, & \frac{1-\beta}{2T}\le\lvert f\rvert\le\frac{1+\beta}{2T}\\ 0 & \text{Otherwise}\end{cases}$ |

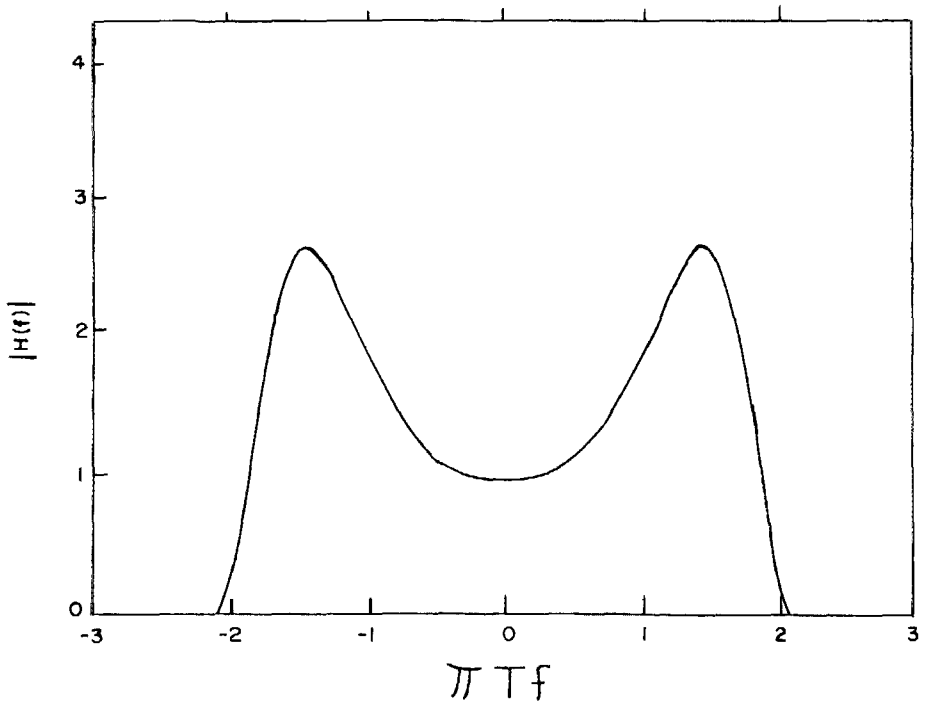


FIG. 4. Plot of the function $|H(f)|$ vs $f$ for $\gamma = 1.5r_0$, $\beta = 0.3$ and $RC = T/10$.

$$\text{SNR} = \frac{4\eta P_0 T r_{\parallel}^2 r_{\perp}^2}{e(r_{\parallel}^2 + r_{\perp}^2)}(1/\xi), \tag{20}$$

where

$$\xi = \frac{1}{\pi}\int_0^{\pi(1+\beta)/2} \frac{\exp[2(r_0 x/\gamma)^2]}{(\sin x/x)^2} \times \begin{cases} 2, & x \le \frac{\pi}{2}(1-\beta) \\ \frac{1}{2}\left\{1 - \sin\left[\left(x - \frac{\pi}{2}\right)/\beta\right]\right\}^2, & x > \frac{\pi}{2}(1-\beta) \end{cases} dx.$$

For a given set of system parameters $\beta$ can be chosen to minimize $\xi$. The minimum value of $\xi$ for large $\gamma/r_0$ is 1.12 (at $\beta = 0.87$). In the limit of large $\gamma/r_0$ therefore the SNR in Eq. (20) is only 0.5 dB below the optimum SNR in Eq. (9). A logarithmic plot of $1/\xi$ vs $\gamma/r_0$ for the optimum $\beta$ is shown in Fig. 5. (The optimum $\beta$ is also shown in the figure.) According to this curve one loses about 1.2 dB in going from large $\gamma$ to $\gamma = 3r_0$. At the cost of another 4 dB one can further reduce $\gamma$ to $1.5r_0$. Compare these figures with the corresponding numbers obtained from the optimum curve of Fig. 2, namely 0.15 and 1.3 dB, respectively.

## IV. CONCLUDING REMARKS

Three methods of data reconstruction from a magneto-optical storage medium with intersymbol interference were discussed. The performance of each method at different storage densities was evaluated on the basis of the signal-to-noise ratio degradation below the maximum level. It was found, for example, that a linear filter with high frequency enhance-

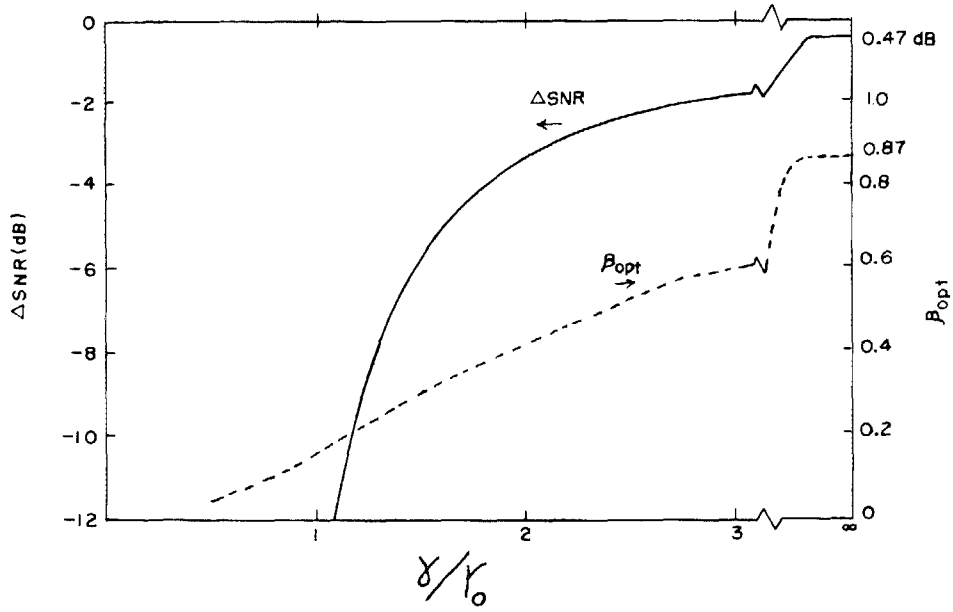


FIG. 5. Logarithmic plot of the function $1/\xi$ vs $\gamma/r_0$ for optimum $\beta$. The broken curve is a plot of $\beta_{opt}$.

ment can be used to reconstruct data stored at $\gamma = 1.5r_0$ at a cost of 5.5 dB in SNR. This is only 4 dB below the SNR of the optimum system. At smaller values of $\gamma$ reconstruction is still possible although SNR degradation become quite severe. At $\gamma = r_0$, for example, the cost in SNR is 14 dB, which is 11 dB below optimum.

## ACKNOWLEDGMENTS

The author is grateful to Dr. Neville Connell of Xerox Corporation and Dr. David Treves of the Weizmann Institute of Technology for many helpful discussions. The project is supported by the National Science Foundation grant number ECS-8307928, and in part by the IBM corporation.

[1]R. M. White, IEEE Spectrum **12**, 32 (1983).
[2]A. E. Bell, Comput. Des. **8**, 133 (1983).
[3]P. Chaudhari, J. J. Cuomo, and R. J. Gambino, Appl. Phys. Lett. **22**, 337 (1973).
[4]M. Mansuripur, G. A. N. Connell, and J. W. Goodman, J. Appl. Phys. **53**, 4485 (1982).
[5]M. Mansuripur, G. A. N. Connell, and J. W. Goodman, Proc. SPIE Conf. **329**, 215 (1982).
[6]A. Papoulis, *Probability, Random Variables, and Stochastic Processes* (McGraw-Hill, New York, 1965).
[7]S. D. Personick, Bell Syst. Tech. J. **52**, 843 (1973).